High speed ciné laser interferometry technique for microlayer studies in boiling

H. G. MacGregor* and H H Jawurek**

(Received in Final form June 1991)

Abstract

During nucleate boiling thin liquid films (microlayers) form beneath the base of bubbles and evaporate into the bubble interiors. An optical technique is described and validated which permits the simultaneous determination of microlayer geometry versus time and the contribution of microlayer evaporation to bubble growth and to boiling heat transfer. Boiling takes place on an electrically heated, transparent tin-oxide coating deposited on a glass plate which forms the floor of the boiling vessel. With laser illumination from beneath the microlayers reflect interference patterns similar to Newton's rings. The fringe patterns are recorded by high-speed ciné photography. Simultaneously, and on the same film, bubble profiles (and thus volumes) are obtained under white light illumination. Problems concerning calibration, fringe interpretation, and the nature of the error in previous non-laser interferometry studies are identified and resolved. Sample results are presented and discussed.

Nomenclature

C	Constant in equation (1)
d	microlayer thickness, m
d_0	initial microlayer thickness, m
m	fringe order
$n_{0/1/2/3}$	refractive index of vapour/liquid/tin oxide film/glass
t_G	bubble growth time, s
V	fringe visibility (contrast)
$\bar{x}$	optical path difference ($= 2n_1d$), m

Greek symbols

λ	wavelength of light in vacuum, m
υ	kinematic viscosity of liquid, m^2/s
ρ_1, ρ_2	fringe reflectances
ρ_{max}, ρ_{min}	maximum and minimum reflectances

Background and aims

During nucleate boiling vapour bubbles form at nucleation sites, grow and detach from (or recondense onto) the heating surface. Because of the rapid initial growth of the vapour phase, the bubble lip 'overtakes' the liquid that is retarded by viscous forces at the heating surface. A thin liquid film, the 'microlayer', is thus formed beneath the bubble base and subsequently evaporates into the bubble interior (Figure 1). Nucleate boiling exhibits very high heat transfer coefficients and has therefore been extensively studied. The interrelation of bubble dynamics and microlayer behaviour, however, remains incompletely understood. The present study aims to present a technique capable of clarifying the role of the microlayer in bubble growth and in boiling heat transfer.

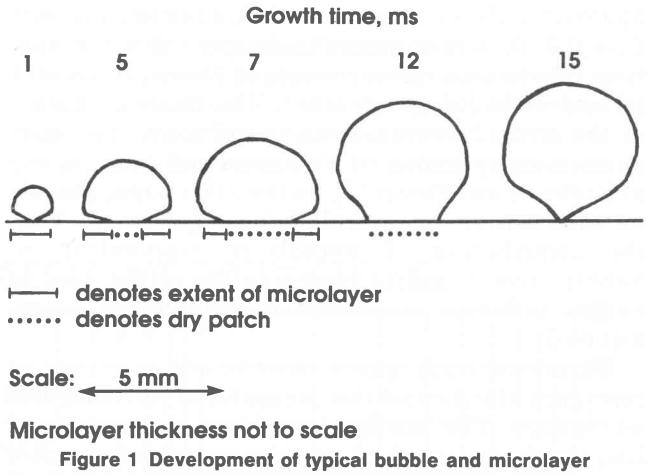

Figure 1 Development of typical bubble and microlayer

The existence of microlayers was postulated by Snyder and Edwards in 1956 [1]. Various surface microthermometry studies, notably that of Cooper and Llod [2] confirmed this hypothesis and provided much insight into microlayer behaviour. The temperature measurements, coupled with boundary layer analysis, suggested that microlayers are wedge shaped in profile, essentially stagnant, and have initial (unevaporated) thicknesses that are given by:

$$d_0 = C(\upsilon t_G)^{05} \qquad (1)$$

Here d_0 is the initial microlayer thickness at bubble base radius r, υ is the kinematic viscosity of the liquid, and t_G is the growth time of the bubble base to attain radius r. The empirical constant C was evaluated at 0,5 to 1,0. Typical microlayer edge thicknesses were of the order of a few micrometers (μm). On further analysis these findings suggested that microlayer evaporation might be a significant contributor both to bubble growth and to the total rate of heat transfer from the area of bubble influence.

* Consulting Engineer, formerly PhD student
** Senior Lecturer,
School of Mechanical Engineering
University of the Witwatersrand, Johannesburg (Fellow)

Visual evidence of the existance of microlayers was first obtained by Sharp [3]. Direct measurements of microlayer geometry versus time were attempted using interference effects similar to Newton's rings, coupled with highspeed ciné photography, on bubbles flattened between a heating surface and a parallel observation window. Jawurek [4] and Judd [5] extended this technique to freely-growing bubbles, the interference fringes being recorded from beneath through transparent heating surfaces. The three studies [3-5] yielded microlayer thicknesses of at least an order of magnitude lower than those deducted indirectly by Cooper and Lloyd [2] and as predicted by equation (1). In all cases the interferometry beams had been produced by arc lamp and line filter arrangements. Voutsinos and Judd [6], however, on repeating this work, but using laser illumination, obtained microlayer thicknesses roughly in agreement with those of Cooper and Lloyd [2]. Koffman and Plesset [7] re-examined the laser interferometry technique and largely confirmed its validity. In applying it to small rapidly growing bubbles in subcooled boiling they obtained microlayer thicknesses approximately in agreement with equation (1) with $C = 0{,}3$. It is now generally accepted that the non-laser interference measurements of Sharp [3] Jawurek [4] and Judd [5] are in error. The cause or nature of the error, however, remains unknown. The laser interferometry studies of Voutsinos and Judd [6] and of Koffman and Plesset [7], on the other hand, provide no information on overall bubble geometry. Thus the contribution of microlayer evaporation to bubble growth and to heat transfer in the area of bubble influence could not be established unambiguously.

The present study aims to describe and to analyse an experimental technique that is capable of providing this information. The technique combines high-speed ciné laser interferometry which provides microlayer geometry (and thus evaporation rates) with conventional high-speed cinématography which simultaneously records overall bubble geometry (and thus volume) versus time. An additional, and equally important, aim of this study is to establish – and learn from – the nature of the error in the non-laser interferometry work [3-5] discussed above.

Heater and boiling vessel

The heating surface consisted of a glass disc (Figure 2) coated with an electrically conducting, transparent film of stannic oxide [8]. The film was in contact with the test liquid and heated by direct current. Silver current leads were attached by indium soldering [9]. The contacts and all leads were coated with silicone rubber sealer.

Discs were cut from ready-coated sheets of the commercial product 'Electropane' of the Libbey Owens Ford Glass Company. The stannic oxide had an optical thickness of half a wavelength, a refractive index of 2,00, and a specific surface resistance of 70 ohms. Film along the edges was removed chemically [10] to produce an H-shaped heater. This reduced bubble formation at the edge of the contacts.

Naturally-occurring (or artificially produced) imperfections in the film acted as bubble nucleation sites. Bubble size was dependent on system pressure. Nucleation density was a function of heat input. The overall heat flux over the central uniformly heated section (see [4]) was obtained from measurements of the electrical input.

The surface performed well with many organic liquids. Water, however, could not be boiled, despite various precautions, the film being destroyed by electrolytic corrosion.

The disc formed the floor of a cylindrical boiling tank. A flat-sided water jacket enveloping the vessel provided a constant temperature bath and eliminated distorion of the bubble profile view.

Reduced pressures could be maintained in the vessel by a vacuum pump and controller arrangement. Two thermocouples established the bulk liquid temperature.

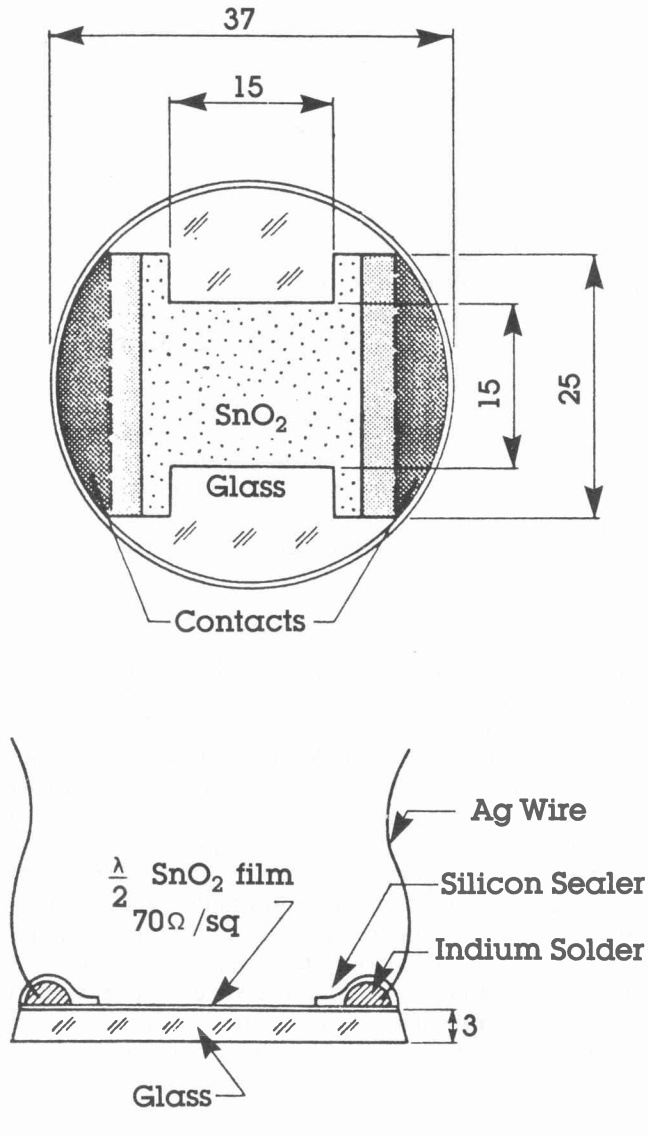

Figure 2 Heating surface

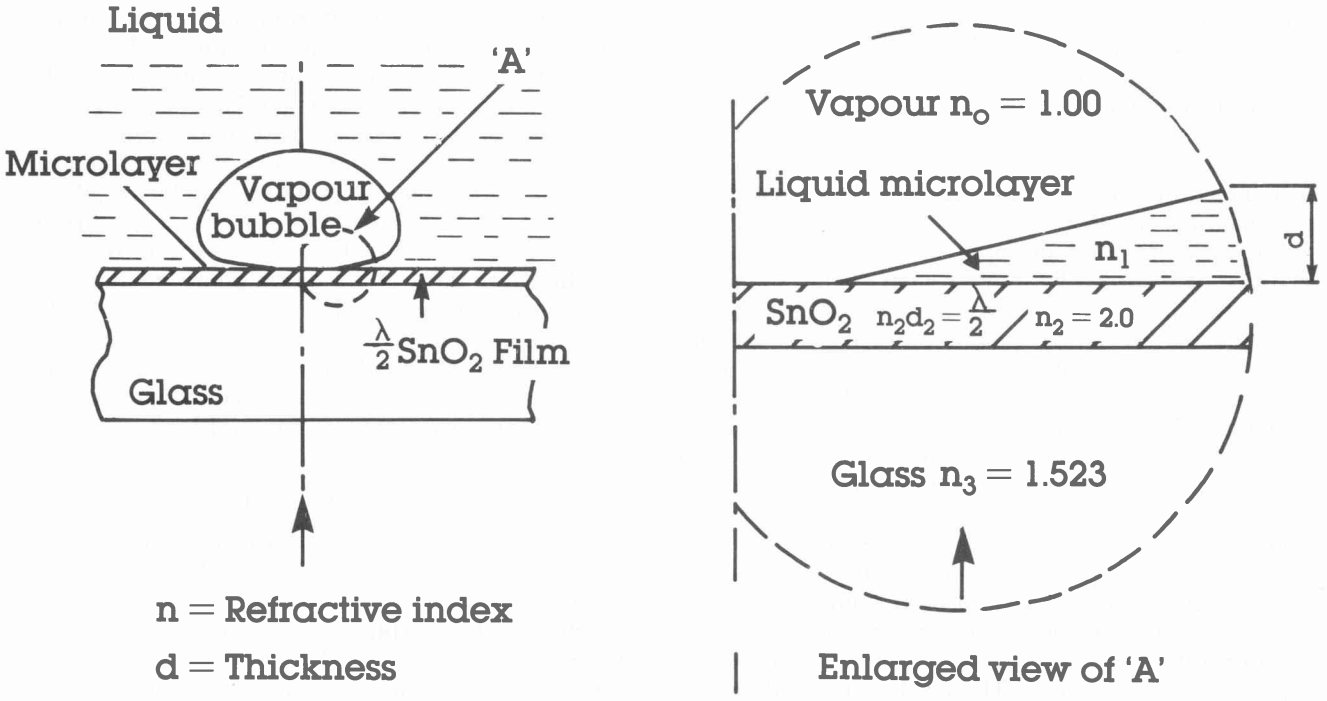

Figure 3 Optics of microlayer interferometry

Optics of microlayer interferometry

Analysis of Fringes

Consider an attached bubble with a partially evaporated microlayer (Figure 3). The system is illuminated from beneath by a normally incident, coherent beam of wavelength, λ. Partial reflections downwards from the upper and lower surfaces of the microlayer give rise to interference fringes by amplitude division, similar in principle to Newton's rings.

In analysing this system, four adjacent optical media, numbered 0 to 3 (as subscripts) in Figure 3, are considered, with media 1 and 2 treated as thin films. Two extreme cases of reflectance, ρ, arise.

Case 1 The microlayer optical thickness is zero or an even multiple of a quarter wave:

$$n_1 d = 2m(\lambda/4) \qquad m = 0, 1, 2 \ldots \tag{2}$$

i.e. the path difference $\bar{x} = 0, \lambda. 2\lambda \ldots$ The reflectance is then given by [11]

$$\rho_1 = [(n_3 - n_0]/(n_3 + n_0)] \tag{3}$$

which is independent of the refractive indices of the two thin films.

Case 2 The microlayer optical thickness is an odd multiple of a quarter wave:

$$n_1 d = (2m + 1)(\lambda/4) \qquad m = 0, 1, 2 \ldots \tag{4}$$

i.e. the path difference $\bar{x} = \lambda/2, 3\lambda/2, 5\lambda/2 \ldots$ The reflectance is then given by [11]

$$\rho_2 = [(n_1^2 - n_3 n_0)/(n_1^2 + n_3 n_0)]^2 \tag{5}$$

which is dependent on the refractive index of the test liquid n_1. (The above treatment of reflectance is, despite appearances, identical to that given in our preliminary report [12], but less cumbersome.)

The refractive index of the chosen test liquid methanol is 1,31 (± 1,5% over the prevailing temperature ranges). Substitution of this value and of the refractive indices shown in Figure 3 into equations (3) and (5) yield $\rho_1 = \rho_{max} = 0{,}043$ and $\rho_2 = \rho_{min} = 0{,}0036$. Equation (2) thus defines maxima of reflectance (light fringes) and equation (4) minima (dark fringes). The fringe visibility, or contrast, given by

$$V = (\rho_{max} - \rho_{min})/(\rho_{max} + \rho_{min}) \tag{6}$$

is then 0,85 which is excellent.

A step from one light or dark fringe to the next (a unit increment in fringe order, m) thus corresponds to an increment of microlayer thickness, d, of 196,4 nm.

Complicating factors

A number of problems regarding fringe analysis and interpretation remain to be considered. First, since laser illumination has a coherence length of the order of centimetres, the glass substrate behaves as a thin film and reflects stationary interference fringes. These fringes appeared as broad, slightly disturbing 'noise fringes' superimposed upon the microlayer fringes (Figure 6). The elimination of such noise fringes is possible in principle, but proved only partially successful in practice [13].

Secondly, the bubble itself constitutes a thin film with reflections from the dome interfering with those from its base. However, since the increase in bubble dome radius during the period of one photographic exposure is interferometrically significant (in the present study at least 1 μm, that is five fringe orders, during the 50 μs exposure),

the 'bubble fringes' are lost by blurring. (The microlayer fringes, moving more slowly by three to four orders of magnitude, are 'frozen'.)

Thirdly, inferference effects between the upper surface of the microlayer and the lower surface of the glass substrate are possible. Very faint 'ghost fringes', possibly attributable to this cause, were occasionally observed, but presented no problem.

Finally, there exists an upper limit to the wedge angle that can be recorded by interferometry. This angle was established during calibration tests as 1° and corresponded to the limit of spatial resolution of fringes at the film plane. The steepest microlayer profile angles that were observed in this study were 0,6°, well within the limit of resolution. The possibility exists, however, of blunting – by preferential evaporation – of the inner (initially thin) microlayer edge. If the resulting tip angle had exceeded 1°, fringes would have been lost and erroneous profiles would have been deduced. While no evidence of such blunting (for example, 'piling up' of inner fringes) was found, its absence could not be proved. Numerical experiments were thus conducted with the microlayer profiles interpreted first normally, and then with the insertion of hypothetical 'lost' fringes. The total evaporated microlayer vapour volume was found to be not very sensitive to such fringe loss. The reason for this is purely geometrical and is analysed in detail in [13]. Thus even if such fringe loss had occurred (for which there is no evidence) the main results of this study would not be seriously compromised.

Calibration

Koffman and Plesset [7] checked the accuracy of the interferometry technique against a calibrated steel ball resting centrally on a transparent heating surface. With the optical system adjusted and operated as in boiling tests, the fringe pattern was recorded and this yielded the geometry of the sphere. Errors in radius of curvature ranging from 2 to 10% were obtained. This is puzzling since interferometry is widely used in the calibration of radii of curvature.

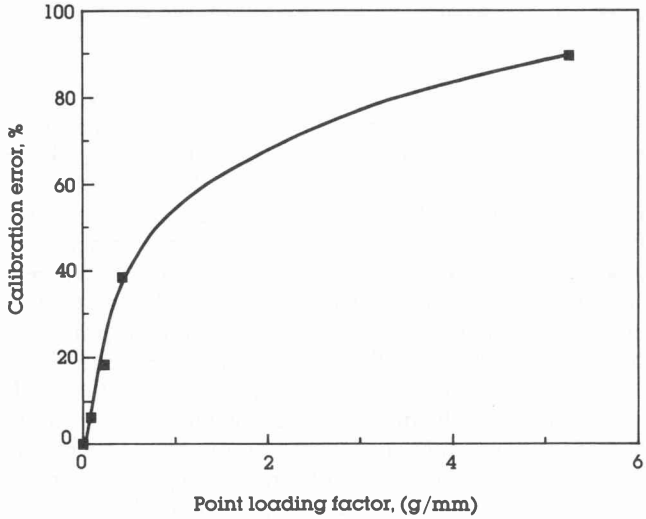

Figure 4 Calibration error

Similar tests were conducted in the present study, initially on a steel sphere 25,4 mm in diameter. The error in the interferometrically determined radius of curvature was 90% (at the outermost fringe). The test was repeated on four further glass or plastic lenses of different sizes and curvatures. Widely differing errors resulted. The errors were then plotted against 'point loading factor', defined as the ratio of mass (g) to radius of curvature (mm) of the calibration objects. Figure 4 shows the error to fall smoothly from 90% at 5,3 g/mm point loading to less than 0,5% at 0,003 g/mm. The apparent errors were thus due to deflection of the heating surface. The thicknesses between the substrate and the calibration object were correctly determined. The same must hold for the microlayer which, in any event, imposes no point load.

Optical system

This is shown schematically in Figure 5. The interferometry beam was produced by a Coherent Radiation CR2SG, two watt argon ion laser, tuned to its most powerful line (λ = 514,5 nm) and fitted with a spatial filter/beam expander unit. Front surface mirror 1 deflected the beam to impinge normally onto the bottom of the heater disc. A beam splitter directed the reflected beam towards a Hadland Hyspeed 16 mm rotating prism camera, the lense of which had been removed. Despite the non-localised nature of the fringes, the camera was focussed on the plane of the microlayer using a separately mounted converging lens. Focussing was necessary for the scaling process (immediately preceeding each run) during which a small glass ruler, resting on the heater, was photographed under diffuse white illumination.

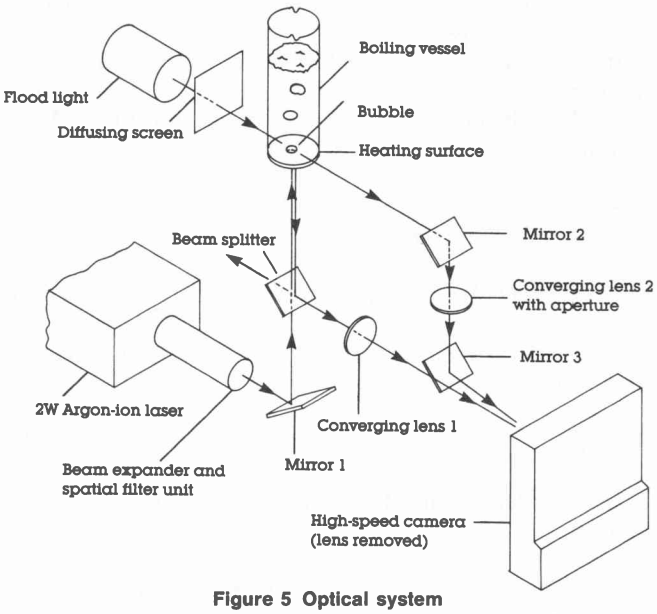

Figure 5 Optical system

Bubble profiles were photographed with diffuse back-illumination. Front surface mirrors 2 and 3, and a further converging lense were so arranged that the bubble profile view and the microlayer interferogram appeared side by side on each frame of film. An f/16 apperture ensured sufficient depth of focus of the profile view. Linear mag-

nification was determined simultaneously with that of the fringe pattern. A rod of known diameter resting vertically on the bubble nucleation site served as scaling object.

The microlayer pattern, containing fine structure, was imaged at a magnification of 1,7X on the film. The magnification of the bubble profiles was 0,6X. The two images were recorded at 4 000 frames per second at exposure times of 50 μs onto Kodak 7250 Video News colour reversal film. The camera provided timing marks at 10 ms intervals at the edge of the film.

Sample results and discussion

A print of one frame of ciné film is shown in Figure 6. The lower left corner shows the profile of the attached bubble, the right hand portion shows the microlayer fringes. The light and dark blotches are the noise fringes previously mentioned. The diagonal line is an optical flow within the glass.

Ciné frames were analysed under projection at a magnification of 90X (film to screen). Analysis were restricted to the first five frames of each bubble cycle and to every fourth or fifth subsequent frame.

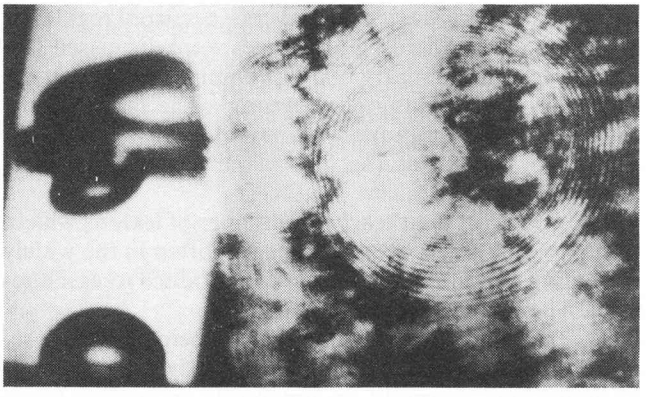

Figure 6 Sample frame of ciné film. Test liquid methanol, overall heat flux 27,8 kW/m², pressure 58,5 kPa, bulk liquid (saturation) temperature 51,2 °C, mean heating surface temperature 76,5 °C.

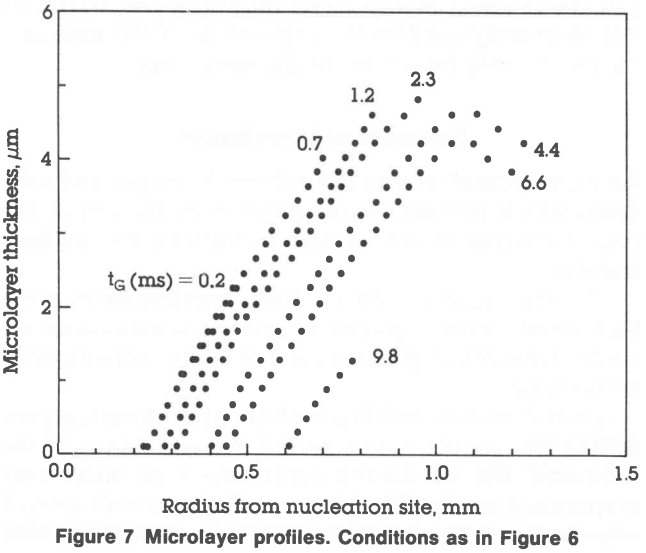

Figure 7 Microlayer profiles. Conditions as in Figure 6

A sample microlayer profile history is shown in Figure 7. (In the interest of clarity only 7 out of a total of 13 analysed profiles are plotted.) Microlayer thicknesses in this and numerous further tests were of the same order as those of Voutsinos and Judd [6] and of Koffman and Plesset [7]. The microlayer growth constant, C in equation (1), was 0,27, in agreement with the values of Koffman and Plesset [7].

In the absence of flow within the microlayer, incremental reductions in its volume (thinning) correspond to increments of microlayer vapour evolution. The cumulative microlayer vapour evolution is shown versus time in Figure 8. Also shown is the bubble volume history, the latter deriving from the analysis of the bubble profiles. It will be noted that the contribution of microlayer evaporation to bubble growth is significant, accounting for 41% of the bubble detachment volume. To the best of our knowledge this contribution has not been previously established by measurement, earlier studies having, to varying extent, relied on indirect or conjectural argument.

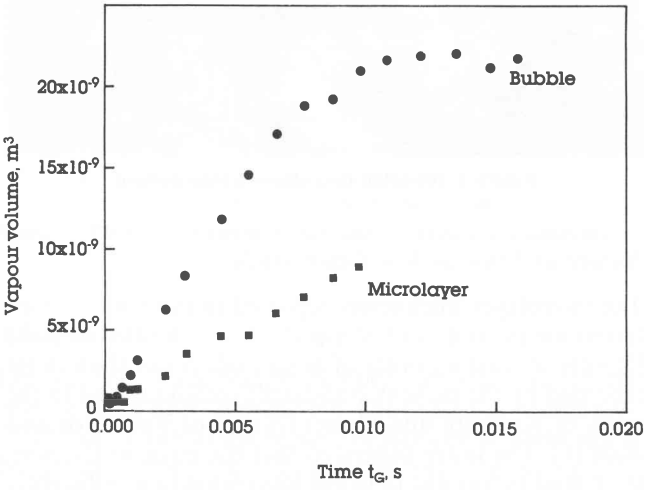

Figure 8 Contribution of microlayer evaporation to bubble growth. Conditions as in Figures 6 and 7

The technique furthermore permits the evaluation of the contribution of microlayer evaporation to total heat transfer from the area of bubble influence. The latter is defined as that portion of the heating surface the heat transfer from which is affected by bubble action. Schlieren studies, for example [14], show the diameter of this area to be approximately twice that of the bubble at maximum volume. The total heat transfer per area of bubble influence thus follows from the bubble profile records and from measurement of the overall energy input to the heater. Microlayer evaporation heat transfer follows from the measurement of vapour evolution, discussed above. For the bubble here considered the microlayer contribution to the total area-of-influence heat transfer was 8,8 or 10,1% (depending on the definition of bubble period [13]).

Finally, the technique lends itself (with suitable numerical processing) to the determination of instantaneous microlayer evaporation heat flux. For the bubble under consideration the heat flux exhibited an initial peak of an astonishing 15,5 MW/m² and then fluctuated about a

value of 0,33 MW/m². The overall mean flux was 0,46 MW/m².

It should be noted, however, that interferograms having the quality and 'analysability' of that shown in Figure 6 were not obtained routinely, test after test, and bubble after bubble. Patterns too distorted, confusing or indistinct to permit analysis were recorded as frequently as those that were satisfactory. An example of a distorted pattern is shown in Figure 9. The interferometry technique is thus selective in permitting the study of regular, well-behaved bubbles only.

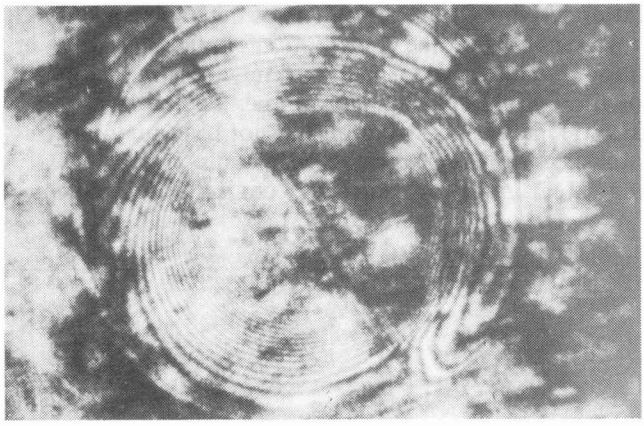

Figure 9 Distorted microlayer fringe pattern

Nature of Error in Non-Laser Studies

The microlayer thicknesses reported in the non-laser interferometry studies of Sharp [3], Jawurek [4], and Judd [5] were at least an order of magnitude lower than those recorded by the present (validated) technique and in the work of Koffman and Plesset [7] and of Voutsinos and Judd [6]. The latter suggested that the error in the non-laser-studies was due to fringe loss owing to insufficiently monochromatic illumination. Insufficient monochromaticity, however, would have led to a fringe pattern decreasing in visibility with increasing fringe order (film thickness), with ultimate loss of the outer fringes. No such effect was observed. Sharp [3] and Jawurek [4] recorded a small number of broad fringes of constant visibility, in the case of the latter extending over the entire bubble base. (The photograph presented by Judd [5] is too indistinct to permit comment.)

An alternative, and more likely, cause of the above error is insufficient resolution at the film plane coupled with the phenomenon of 'fringe bunching'. The lack of resolution may have been caused by insufficient magnification (this was 0,55X in [4], as opposed to 1,7X in the present study), or to focussing errors. The latter can easily arise with low-coherence (non-laser) illumination which leads to localised fringes (laser illumination produces non-localised fringes that are 'everywhere in focus'). Fringe bunching is demonstrated with particular clarity in the work of Katto and Shoji [15] which deals with microlayers on injected air bubbles. Their interferograms show fine fringes bunched in groups of roughly 10, with the groups separated by a broader fringe. (This implies that the upper microlayer surface was wavy or step-shaped rather than smooth.) If these interferograms are viewed with the resolution of the eye deliberately reduced by defocussing, they appear very similar to the patterns recorded by Sharp [3] and Jawurek [4]. A re-examination of the ciné records of the present study showed occasional cases of fringe bunching, and these generally occurred with large bubbles. (An example of mild bunching is to be seen in the upper right-hand region of Figure 9.) The large bubble size (maximum diameters of 10 to 17 mm) in the study of Jawurek [4] would thus appear to have favoured the formation of wavy microlayers and thus the occurrence of fringe bunching. In short, it is suggested that the broad 'fringes' observed in the non-layer studies [3-5] were groups of unresolved real fringes.

If the above explanation is correct, then normal microlayers having a nonwavy upper surface would have yielded interferograms showing no fringes pattern at all. Such cases certainly occurred in numerous preliminary tests conducted by Jawurek. (We limit consideration to the latter study on the grounds of insufficient familiarity with the background to [3] and [5].) When concentric ring patterns were recorded (as expected) these were seized upon as 'results at last'! The study then steered itself imperceptibly into a region of conditions where such ring patterns – in reality unresolved groups of fringes caused by wavy microlayers – occurred regularly. Occasional tests yielding no fringes were dismissed (together with the similarly blank preliminary runs) on the grounds of 'something gone wrong'. The fact that the interferometry technique was limited by the spatial resolution of fringes at the film plane was simply overlooked.

The above account teaches a number of lessons which, though well known, are apt to be forgotten in the widely prevailing conditions of pressure to produce research results. The lessons are the following:

An experimental technique, before being applied, requires to be analysed in detail, particularly with regard to its limitations. Secondly, an apparently anomalous result (here a blank interferogram) may not be shrugged off and left unexplained. If it is to be attributed to an experiment 'gone wrong', the nature of what went wrong must be established. Finally, the repeated measurement of the same effect, even by different investigators (in the present case the sub-micron microlayer thicknesses in [3-5]) does not necessarily confirm the correctness of the measurements. All may be subject to the same error.

Summary and conclusions

An experimental technique has been developed and validated which permits the quantitative evaluation of the role of microlayer evaporation in nucleate boiling heat transfer.

The technique combines laser interferometry with high-speed cinématography to provide simultaneous records of microlayer geometry and of bubble volume, both versus time.

It was demonstrated that with suitable numerical processing the above records permit the evaluation of the following: the volumetric contribution of microlayer evaporation to overall bubble growth, the contribution of microlayer evaporation to total heat transfer in the area

of bubble influence, and the instantaneous microlayer evaporative heat flux.

A plausible explanation was given of the nature (and manner of occurrence) of the error in previous non-laser interferometry studies. Technically, the error appears to have been caused by insuficient spatial resolution at the film plane. More fundamentally, however, it seems that the error was due to the unconscious violation of the principles of research.

Acknowledgements

This study was supported by the Richard Ward Endowment Fund, University of the Witwatersrand, Johannesburg. Additional funding was provided by the Postgraduate Bursary schemes of the CSIR and the University, and by the Foundation of Research Development. The authors wish to thank the trustees and councils of these bodies for their generous support.

References

1. Snyder, N. W. and Edwards, D. K., In: 'Summary of Conference on Bubble Dynamics and Heat Transfer'. Jet Propulsion Laboratory Memo. Non. 20-137, 1956.
2. Cooper, M. G. and Lloyd, A. J. P., 'The Microlayer in Nucleate Pool Boiling', International Journal of Heat and Mass Transfer, Vol. 12, 1969, pp. 895-913.
3. Sharp, R. R., 'The Nature of Liquid Film Evaporation During Nucleate Boiling', NASA Technical Note, TN D-1997, 1964.
4. Jawurek, H. H., 'Simultaneous Determination of Microlayer Geometry and Bubble Growth in Nucleate Boiling', International Journal of Heat and Mass Transfer, Vol. 12, 1969, pp. 843-848.
5. Judd, R. L., 'Comparison of Experimental Microlayer Thickness Results'. Transactions of the Canadian Society of Mechanical Engineering, Vol. 1, 1972, pp. 168-170.
6. Voutsinos, C. M. and Judd, R. L., 'Laser Interferometric Investigation of the Microlayer Evaporation Phenomenon', Journal of Heat Transfer, Vol. 97, 1975, pp. 88-92.
7. Koffman, L. D. and Plesset, M. S., 'Experimental Observations of the Microlayer in Vapor Bubble Growth on a Heated Solid', Journal of Heat Transfer, Vol. 105, 1983, pp, 625-632.
8. Aitchison, R. E., 'Transparent Semi-Conducting Oxide Films'. Australian Journal of Applied Science, Vol. 5, 1954, pp. 10-17.
9. Belser, R. B., 'A Technique of Soldering to Thin Metal Films'. Review of Scientific Instruments, Vol. 22, 1954, p. 180.
10. Tarnopol, M. S., 'Treatment of Films with Liquid', U.S. Patent 2 606 566, 1952.
11. Vasicek, A., 'Optics of Thin Films'. North Holland, Amsterdam, 1960, p. 176.
12. Jawurek, H. H., MacGregor, H. G. and Bodenheimer, J. S., 'Microlayer Topology and Bubble Growth in Nucleate Boiling'. Proceedings 17th International Congress on High Speed Photography and Photonics. Vol. 1, 1986, pp. 202-211.
13. MacGregor, H. G., 'Microlayer Evaporation in Nucleate Boiling', PhD Thesis, University of the Witwatersrand, Johannesburg, 1987.
14. Hau, Y. Y. and Graham, R. W., 'Analytical and Experimental Study of the Thermal Boundary Layer Ebullition Cycle in Nucleate Boiling', NASA Technical Note, TN D594, 1961.
15. Katto, Y. and Shoji, M., 'Principal Mechanism of Micro-Liquid-Layer Formation on a Solid Surface with a Growing Bubble in Nucleate Boiling', International Journal of Heat and Mass Transfer, Vol. 13, 1970, pp. 1299-1311.

Note: Reference 12, above, is a preliminary report on the work presented in this paper.